KERNFORSCHUNGSZENTRUM

KARLSRUHE

Juli 1969

KFK 1017
EUR 4180 e

Institut für Angewandte Reaktorphysik

Irradiation-Induced Biaxial Creep Behaviour of Fuel-Element Claddings for Fast Reactors: Experimental and Theoretical Results

H.J. Laue, K.D. Closs, M. Guyette

GESELLSCHAFT FÜR KERNFORSCHUNG M.B.H.

KARLSRUHE

KERNFORSCHUNGSZENTRUM KARLSRUHE

Juli 1969

KFK 1017
Eur 4180 e

Institut für Angewandte Reaktorphysik

Irradiation-Induced Biaxial Creep Behaviour of Fuel-Element Claddings for Fast Reactors: Experimental and Theoretical Results *

H.J. Laue, K.D. Closs, M. Guyette **

Paper presented at the IAEA Symposium on Radiation Damage in Reactor Materials, Vienna, 2 - 6 June 1969

Gesellschaft für Kernforschung mbH, Karlsruhe

* Work performed within the association in the field of fast reactors between the European Atomic Energy Community and Gesellschaft für Kernforschung mbH, Karlsruhe

** Belgonucléaire-Delegate

Content

1. Introduction

The design and optimisation of fuel elements is based on irradiation experiments in which selected alloys are tested under mechanical stress at high temperature and high neutron flux. The real stress of the fuel element cladding cannot be simulated completely by these tests, they only give information about the influence of single test parameters which are independant of each other. The interaction of these different parameters is almost unknown.

On the other hand, the "Fuel-element performance tests" as integrated tests can only show whether a certain fuel element concept is suitable or not, and the individual stresses cannot be measured directly. Such tests are therefore almost useless for the optimisation of fuel elements.

The use of a computer programme may be a possible way for increasing the effectiveness of the different irradiation experiments. Such a computer programme has to take into account the different stresses in a fuel element cladding and has to consider the material properties derived from specific irradiation experiments.

The creep behaviour of the fuel element cladding is most important for the design of a fuel element. It is often described by the Norton's creep law. For the present case, this law is not always sufficient, and it is necessary to take into consideration the influence of a high neutron flux as well as the complex behaviour of precipitations. In [1] Hesketh has introduced a so called internal stress, to describe these phenomenon. It is not yet known, however, whether the interaction of all the different factors can be described sufficiently by this formulation.

A suitable theoretical formulation is absolutely necessary since, for example, only a few results of uniaxial in-pile creep experiments are available, which partly contradict each other. The influence of high neutron fluxes ($>10^{15}$ n/cm^{2}sec) and neutron fluences ($>10^{22}$ n/cm^2) on the in-pile creep behaviour is not yet known and probably can not be determined in the near future for technical reasons. Moreover, the results from uniaxial experiments can only be used limitedly for the multiaxial load of a fuel element cladding.

As a first approximation, creep parameters, determined from the measured tangential strains of irradiated pressure tubes, have therefore been used for the calculations presented here. Thermal stresses in the cladding, a continuous pressure increase due to fission gas release and a reduction of the wall thickness due to corrosion were taken into account for the calculations.

The tested alloys were the German stainless steel 16Cr13Ni, Incoloy 800 and Hastelloy X.

2. Results of the in-pile stress rupture tests

The irradiation of the pressure tubes was performed in the Belgian Material Test Reactor BR2 at Mol. The fast neutron flux was between 2.5 and 4.0 x 10^{14} n/cm^{2}sec (2.0 and 3.5 x 10^{14} n/cm^{2}sec thermal neutron flux) depending on the position of the specimens within the irradiation rig. The irradiation temperature was between 600°C and 700°C, and was kept constant with an accuracy of $\pm$ 1°C by an electrical heater. During irradiation, the specimens had a constant inner pressure. A description of the irradiation equipment has been given in [2].

Some of the results for the German 16Cr13Ni stainless steel and Incoloy 800 have been published earlier [3].

The composition of the test materials is shown in Table 1. The specimens had an outer diameter of 7 mm, a wall thickness of 0.4 mm and a length of 45 mm. The results of the in-pile stress-rupture tests are summarized in Figures 1 to 3. In the upper curves of the figures, the inner pressure of the irradiated and unirradiated specimens has been plotted versus the rupture time, whereas in the lower curves the tangential rupture strain of the pressure tubes can be seen as a function of the rupture time for each material tested.

16Cr13Ni Fig. 1 :

The reduction of the stress rupture strength at 600°C due to the irradiation is about 40 %. For the unirradiated material, the tangential rupture strain obviously increases for increasing values of the time. For the irradiated material, however, this tendency is not evident: the tangential rupture strain is nearly constant and amounts to 0.4 and 0.8 %.

At a temperature of 700°C, the unirradiated material shows a deviation from the linear behaviour in the diagram log stress versus log time. This phenomenon can probably be explained by overaging at this temperature. The decrease of the stress rupture strength is even more pronounced for the material subjected to irradiation. The stress rupture strength is reduced 50 % by irradiation in short time tests (about 150 hrs.) and 55 % in long time tests (about 900 hrs.). In parallel with the strong decrease in the stress rupture strength, an increase in the ductility with time is observed. This behaviour is particularly obvious for the irradiated material. While the tangential strain is only 0.35 % for the short time tests, it increases to 2.5 % for the long time tests (about 900 hrs.). This last value is almost equal to the value obtained for the unirradiated material.

Incoloy 800 Fig. 2 :

At a temperature of 600°C, the stress rupture strength of the test specimens is reduced 20 % and 30 % by irradiation for test time of 200 hrs. and 2000 hrs. respectively.

At 700°C, the reduction is about 30 % for all the specimens and test times. The ductility of the irradiated Incoloy 800 tubes (no Ti and Al) is still high: the tangential rupture strain amounts to 2.5 to 4.7 % at 600°C and 700°C.

Hastelloy X Fig. 3 :

Of all the tested materials, this alloy presents the smallest reduction in stress rupture strength due to the irradiation: at a temperature of 650°C this reduction amounts to about 15 % after 200 hrs. and to about 27 % after 1000 hrs. At 700°C, the reduction of the stress rupture strength due to irradiation is of the same order of magnitude: about 15 % after 100 hrs. and 20 % after 1000 hrs.

The strong decrease of the ductility for increasing test durations is observed for this material in the irradiated as well as in the unirradiated conditions. However, the absolute values of the strains observed for this material are relatively high in comparison with the other alloys investigated here. At 650°C the measured strains of the irradiated material remain always within 2 to 3 %, while at 700°C they decrease from about 7 % to 3 % at 1000 hrs. Moreover, it should be mentioned that for this particular alloy many of the tested tubes burst at 650°C over the whole length, while for the other alloys, the specimens presented small intercrystalline cracks.

From the experimental results, the creep parameters have been determined, and calculations were performed with the computer programme CRASH (CReep Analysis in SHeaths). The basic method used in this programme is first briefly explained.

3. Computer programme CRASH

The computer programme CRASH allows the tri-axial stresses and strains at discrete values of the time in a long, axisymmetric cylinder to be calculated when creep occurs in the material. The calculation neglects the axial temperature gradient (this last one is, in all practical cases, of the order of 1 % of the radial gradient).

With this hypotheses it can be shown that the principal stresses are in the radial, tangential and axial directions, and that the total strain in the axial direction is independent of the radius r.

The equilibrium condition, which is not trivial, is expressed by:

$$\frac{d\sigma_r}{dr} + \frac{\sigma_r - \sigma_\theta}{r} = 0 \qquad (1)$$

while the compatibility equations are written:

$$\varepsilon_r = \frac{du}{dr} \; ; \quad \varepsilon_\theta = \frac{u}{r} \; ; \quad \varepsilon_z = C_3 \qquad (2)$$

Use is made of the following relations between stresses and total strains:

$$\begin{aligned} \varepsilon_r &= \frac{1}{E}\left[\sigma_r - \mu(\sigma_\theta + \sigma_z)\right] + \alpha T + \varepsilon_{cr} \\ \varepsilon_\theta &= \frac{1}{E}\left[\sigma_\theta - \mu(\sigma_r + \sigma_z)\right] + \alpha T + \varepsilon_{c\theta} \\ \varepsilon_z &= \frac{1}{E}\left[\sigma_z - \mu(\sigma_r + \sigma_\theta)\right] + \alpha T + \varepsilon_{cz} \end{aligned} \qquad (3)$$

The equilibrium equation, the compatibility equations and the stress-strain relations are integrated for a determined value of the time under the assumption that the creep strains ε_{cr}, $\varepsilon_{c\theta}$ and ε_{cz} are known functions of the coordinates.

In the integration, three constants appear, which are determined by the following boundary conditions:

$$\begin{aligned} (\sigma_r)_{r=a} &= -p_a \\ (\sigma_r)_{r=b} &= -p_b \\ \int_{r_a}^{r_b} 2\pi\sigma_z \, r \, dr &= F_z \end{aligned} \qquad (4)$$

The solution of these equations allows the stress and the total strain state to be determined for a given time. An iteration process, summarized in Figure 4, allows the calculation of the creep strains. The following steps are successively made:

1 - First estimate of the creep strains.
2 - Calculation of the total strain and of the stress states compatible with these creep strains and the boundary conditions (inner and outer pressure, axial force).
3 - From the average stress state during the time interval, calculation of the creep strains using an arbitrary creep law (for the particular case of the calculations described here, Norton's law was used).
4 - If convergence is not reached, new creep strain estimates are determined by a mathematical method derived from the Newton Raphson method to solve a system of nonlinear equations.

By this method, the thermal stresses are automatically taken into account; indeed in the relations between stresses and strains the thermal strains appear. Also the stress relaxation by creep is automatically taken into account due to the fact that the actual creep strains appear in the relations between stresses and strains.

The boundary conditions (inner and outer pressure, axial force) and the variables, allowing the temperature distribution (coolant temperature, power per unit length) to be determined, can be arbitrary functions of the time.

This allows the actual conditions of a fuel pin cladding to be simulated very exactly.

4. Determination of the creep parameters

A mean creep rate has been determined for the individual specimens from the tangential strains and the test times, and the creep parameters k and n, according to Norton's creep law $\dot{\varepsilon} = k\,\sigma^n$, were calculated for each material and each test temperature by the method of the least square error.

All experimental results could not be used for these calculations, because some tangential rupture strains scattered over a wide range, and the strain could not be measured on specimens which cracked over their whole length.

The calculation of a mean creep rate from the relation rupture strain to rupture life, neglecting the primary and tertiary stage of the creep curve, is allowed as a first approximation [4]. The results from long duration experiments were mainly used for the determination of the creep parameters in order to get a small error by neglecting the primary stage.

The tertiary stage of the creep curve can be neglected for the following reasons:

1. At creep tests under multiaxial stress, the tertiary stage of the creep curve is less marked compared with tests under uniaxial stress, as rod or sheet specimens normally show a higher reduction in area at rupture.
2. It can be seen from many experiments that the He-atoms, formed by thermal and fast (n,α)-reactions, conglomerate under stress at temperatures above 600°C. These bubbles reduce the critical crack length at the grain boundaries, and the first cracks already appear during the secondary stage of creep.

This assumption is verified by the results of the in-pile stress rupture tests reported here. In Fig. 5 you can see the mean creep rate of irradiated Incoloy 800 tubes as a function of the stress. The results for the burst and not burst specimens are on one curve, which shows that the tertiary stage of the creep curve is almost negligible.

The creep parameters for the irradiated and unirradiated specimens, which have been calculated from the relation creep strain to test time, are summarized in table 2. From these creep parameters it can not be concluded whether the creep rate is changed by irradiation or not, because the assumptions mentioned above are not valid for unirradiated specimens.

The creep parameters for the irradiated 16Cr13Ni steel at 700°C are only approximate values, not useful for calculations. According to Figure 1, the creep behaviour cannot be described by a constant k and n all over the experimental time because the stress rupture strength is no linear function of the time in the diagram log stress versus log time.

Introductory calculations have been carried out in order to control the creep parameters. The mean deviation between the calculated and the experimental lifetime at a measured strain was between 5 and 10 %. The maximum deviations were up to 50 %, however these deviations were only observed for specimens having low tangential strains (less than 1 %), as the measurement of these small strains under hot-cell conditions is rather difficult and thus not very accurate.

5. Results of the calculations

5.1. Calculations with constant inner pressure

In the first part of the calculations, the same operating conditions as for the in-pile stress rupture tests were assumed. i.e. a constant inner pressure and a constant temperature throughput the wall of the tubes. The time after which a given strain is reached has been calculated as a function of the inner pressure. These results are plotted in Figures 6 to 8.

16Cr13Ni Fig. 6 :

The tangential rupture strains for tubes of this material are always smaller than 1 %. For this reason the times were calculated when a tangential creep strain of 0.1 or 0.2 % was reached. Moreover, the geometrical dimensions of the fuel pins of the Na-2 reactor [5] were used, i.e. an outer diameter of 6 mm and a wall thickness of 0.38 mm. At 600°C, the curves of the calculated 0.1 and 0.2 % creep strength are almost parallel with the stress rupture strength curves. This can easily be explained, because the rupture strains at 600°C increase very slowly with the test time according to Fig. 1.

Incoloy 800 Fig. 7 :

The material examined showed tangential rupture strains of more than 2 %. Therefore, the 1 and 2 % creep strength has been taken as a basis for the calculations. At 600°C, the stress rupture strength curve is nearly identical with the 2 % creep strain curve since the measured rupture strains amount to 2.8 and 3 %.

At 700°C, there is a bigger difference between the 2 % creep strain curve and the stress rupture strength curve compared with the curves at 600°C, because the measured rupture strains were higher (2.5 to 4.7 %). The curves of the stress rupture strength and the 1 % and 2 % creep strain also run almost parallel. This is due to the fact that the rupture strains did not differ very much with the test time.

Hastelloy X Fig. 8 :

On the basis of the measured strains, the creep strain limits of 1 % and 2 % were also chosen for the calculations reported here. From Fig. 3 it can already be seen that the rupture strains of the investigated Hastelloy X decreased markedly with increasing time. Therefore in Fig. 8, the curves of the stress rupture strength and the 1 % and 2 % strains approach or intersect, i.e. the tubes burst before having reached the theoretically assumed strain. That means that, at 700°C, the 0.5 % creep strength has to be considered for the design of fuel elements with a lifetime higher than 1500 hrs.

The next calculations performed with the computer programme take into account thermal stresses due to a temperature gradient in the wall of the tube. A rod power of 500 W/cm, according to a temperature gradient of about 50°C, was assumed, and the mean midwall temperature was the same as used in previous calculations, when no temperature gradient was assumed. The calculated creep parameters were interpolated or extrapolated for other temperatures in order to get the creep rate and the stresses in the various hot zones of the fuel element cladding.

The reduction of rupture time due to thermal stresses is not very significant because of the small wall thickness of the tubes. The calculations for Hastelloy X showed nearly no influence of thermal stresses on the rupture time, which may be due to the nearly identical creep parameters at 650°C and 700°C. No calculations could be carried out for the 16Cr13Ni steel because the creep parameters at 700°C are not good enough.

The results for Incoloy 800 are plotted in Fig. 9. The maximum reduction of rupture time is about 3.25 %. At 600°C, the curve increases continously with time, whereas at 700°C the reduction of rupture time has a maximum at 1000 hrs. This maximum cannot yet be explained. The relaxation of the thermal stresses as a function of the inner pressure and the time has to be analysed more accurately.

5.2. Calculations with pressure increase

During the operation time of a fuel element in a reactor, the cladding is not stressed by a constant pressure, but the pressure will slowly increase due to the fission gas release. Assuming a pressure increase from 0 to a given end pressure, the lifetime of the fuel element is increased compared with tests at a given constant end pressure.

Fig. 10 shows the results for irradiated Hastelloy X tubes. The time for a tangential strain of 0.5 % is plotted versus the end pressure after a linear pressure increase. For comparison, the curve with constant inner pressure has also been drawn in this diagram.

Assuming an identical end pressure, the operation time is increased by a factor of 7 at 650°C and by a factor of 8 at 700°C. At long times (about 10 000 hrs.) these factors slowly rise. Similar results were found for the calculations with Incoloy 800 and the 16Cr13Ni steel.

Fig. 11 shows the influence of corrosion on the lifetime of fuel element claddings. A mean corrosion rate of 40 µm/yr was assumed for all alloys, and the calculations were also carried out with a linear pressure increase. The lifetimes of the fuel elements are reduced by 14 % to 16 % by corrosion after 15 000 hrs, depending on the test temperature and the materials used.

6. Summary

The results presented here are a first step towards a complete stress analysis of the fuel element cladding of a high-power reactor. Sufficient results from well defined in-pile stress rupture and creep tests are required for such a theoretical analysis. The fast neutron flux should be as high as possible for such experiments.

The calculations carried out up to now show that the complex stresses and strains in a fuel element cladding cannot always be described sufficiently by Norton's creep law $\dot{\varepsilon} = k\,\sigma^n$.

According to the theoretical considerations and some experimental results, the minimum creep rate should not be influenced by irradiation [6]. However, this is only valid for steady diffusion controlled creep, and is no longer evident when structural changes occur. At a fast neutron flux of 5×10^{15} to 1×10^{16} n/cm^{2}sec, the fuel element of a high-power reactor is exposed to a dose larger than 10^{23} n/cm^2 after an operation time of 15 000 hrs. It is an open question whether the assumption mentioned above will be valid for such extreme situations. Böhm [7] mentions that at high neutron fluxes a decrease of the creep rate due to voids and dislocation may be possible. On the other hand a remarkable decrease of the lifetime of the cladding due to high temperature embrittlement by (n,α)-reactions can be noticed. This embrittlement already appears after a neutron fluence of 10^{18} n/cm^2. According to the bubble model [7], the high temperature embrittlement should be reduced at long times under stress. This hypothesis is verified at least by the in-pile stress rupture tests results at 700°C. The absolute value of the embrittlement decreases at long times compared with the unirradiated specimens. Moreover, a decrease of the creep rate with increasing Helium concentration beyond the creep rate of the unirradiated specimens should be noticed, caused by the reduction of the migration of dislocations by He-bubbles [8].

These partly contradictory statements show very clearly that the high neutron dose is the dominating effect. By that it can be understood that the time dependant processes which partly influence each other cannot be described by a simple creep law.

The way described here should be sufficient for a first fuel element concept. As we have seen, neutron irradiation is the predominant effect. The lifetime of the fuel element cladding is reduced by irradiation between 55 % and 15 %, depending on the material used and the test conditions. On the other hand, thermal stresses and a reduction of the wall thickness due to anticipated corrosion have no big influence on the reduction of lifetime, whereas the pressure increase due to fission gas release and swelling of the fuel leads to a remarkable increase of the operation time compared with experiments at constant inner pressure.

Thus future experiments will be concentrated mainly on the effect of irradiation; and theoretical studies will be made, as far as possible, on high temperature embrittlement, void formation, dislocation networks and volume increase.

Acknowledgement

The unirradiated specimens have been tested in the Institute of Material research and Solid state physic The authors thank Mr. H. Kaupa and F. Polifka for the preparation of unpublished test results.

7. References

[1] HESKETH, R.V., Application of the generalized theory of yielding creep in Zirconium alloys, J. nucl. Mat. 26 (1968) 77.

[2] KRAMER, W., SCHMIDT, L., WILL, H., "Bestrahlungseinrichtung zur Hüllmaterialuntersuchung für schnelle Brutreaktoren", Kerntechnik 9 (1967) 499.

[3] LAUE, H.J., BÖHM, H., HAUCK, H., Multi-axial in-reactor stress-rupture strength of stainless steels and a Nickel ally, 71. Annual meeting of the American society for testing and material, 23. - 28. June 1968, San Francisco/Calif., KFK-814.

[4] McCOY, H.E., WEIR, J.R., Stress-rupture properties of irradiated and unirradiated Hastelloy N tubes, Nucl. Applications, Vol. 4 (Febr. 1968) 99.

[5] GAST, K., SCHLECHTENDAHL, E.G. et al., Schneller natriumgekühlter Reaktor Na2 (Oct. 1967) KFK 660.

[6] HESKETH, R.V., Diffusion creep under neutron irradiation, J. nucl. Mat. 29 (1969) 27.

[7] BÖHM, H., Die Porenbildung in metallischen Werkstoffen durch Neutronenbestrahlung (Sept. 1968) KFK 838.

[8] WOODFORD, D.A., SMITH, J.P., MOTEFF, J., Effect of Helium gas bubbles on the creep ductility of an austenitic alloy, J. nucl. Mat. 29 (1969) 103.

Symbols used

a	cladding inner radius
b	cladding outer radius
C_3	integration constant
E	Young's modulus
p_a	inner pressure
p_b	outer pressure
r	radius
T	temperature (function of r)
u	radial displacement
α	thermal expansion coefficient
ε_r	radial total strain
ε_θ	tangential total strain
ε_z	axial total strain
ε_{cr}	radial creep strain
$\varepsilon_{c\theta}$	tangential creep strain
ε_{cz}	axial creep strain
μ	Poisson's ratio
σ_r	radial stress
σ_θ	tangential stress
σ_z	axial stress

ALLOY	WEIGHT - PERCENT									
	C	Cr	Ni	Mo	V	Ti	Al	Fe	Nb/Ta	Co
16 Cr 13 Ni	0.08	16.9	13.6	1.2	0.6			BAL	0.7	
INCOLOY 800	0.016	20.6	31.9					BAL		
HASTELLOY X	0.1	21.9	BAL	9.0				18.3		1.6

Table 1 Nominal composition of Test Materials

ALLOY	TEMPERATURE [°C]	unirradiated		irradiated	
		n	k	n	k
16Cr13Ni	600	6.8	$2.8 \cdot 10^{-15}$	7.5	$9.8 \cdot 10^{-15}$
	700	3.2	$1.8 \cdot 10^{-8}$	[4.8]	$[2.5 \cdot 10^{-9}]$
INCOLOY 800	600	6.8	$1.4 \cdot 10^{-11}$	6.9	$4.2 \cdot 10^{-12}$
	700	6.5	$3.4 \cdot 10^{-9}$	4.9	$8.1 \cdot 10^{-8}$
HASTELLOY X	650	9.8	$2.5 \cdot 10^{-16}$	5.5	$2.2 \cdot 10^{-11}$
	700	7.4	$2.9 \cdot 10^{-12}$	6.4	$2.2 \cdot 10^{-11}$

Table 2 Creep Parameters of Test Materials

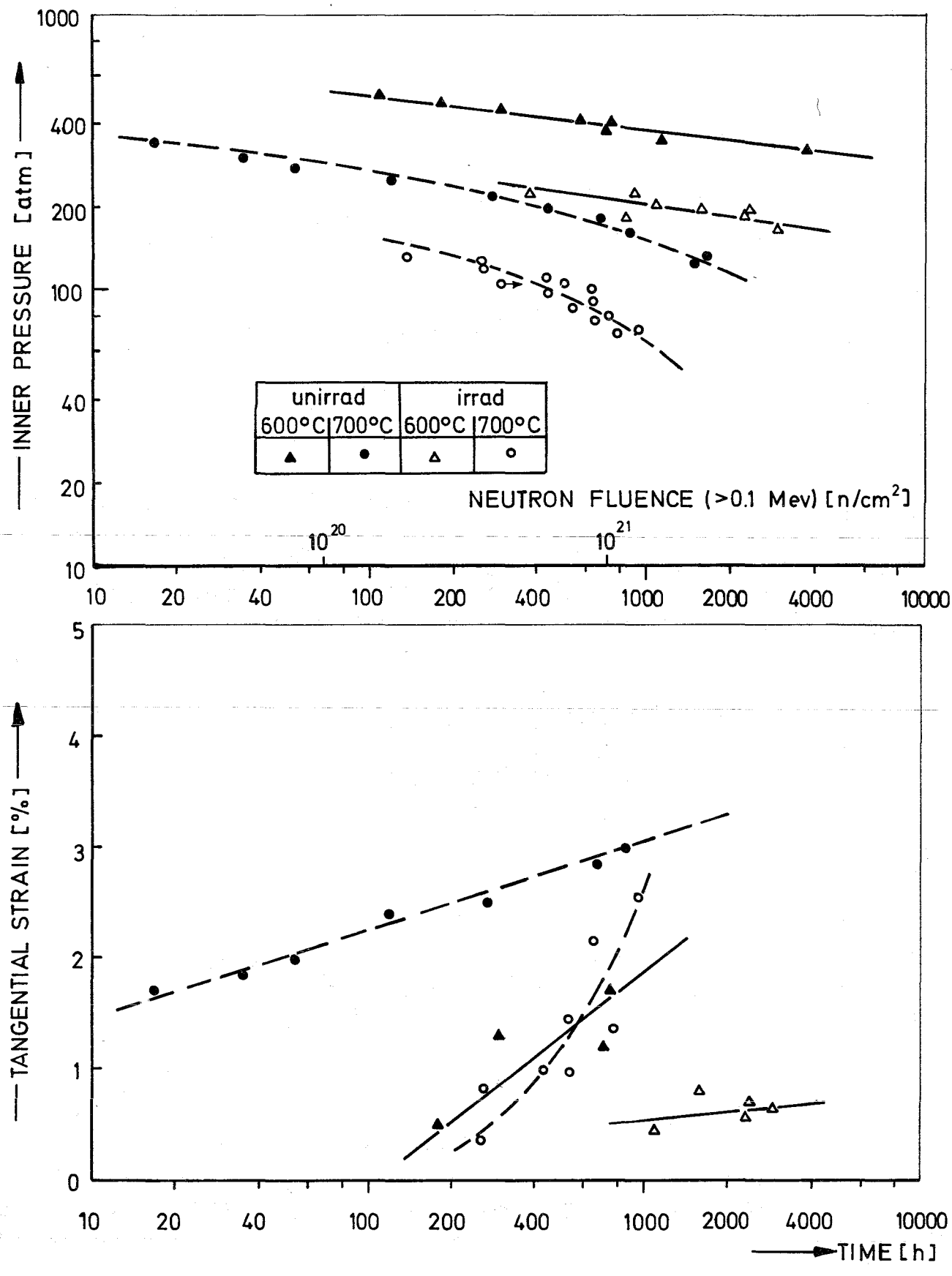

Fig. 1 Stress rupture strength and tangential rupture strain of 16 Cr 13 Ni tubes

Outer diameter 7mm Wall thickness 0.4 mm

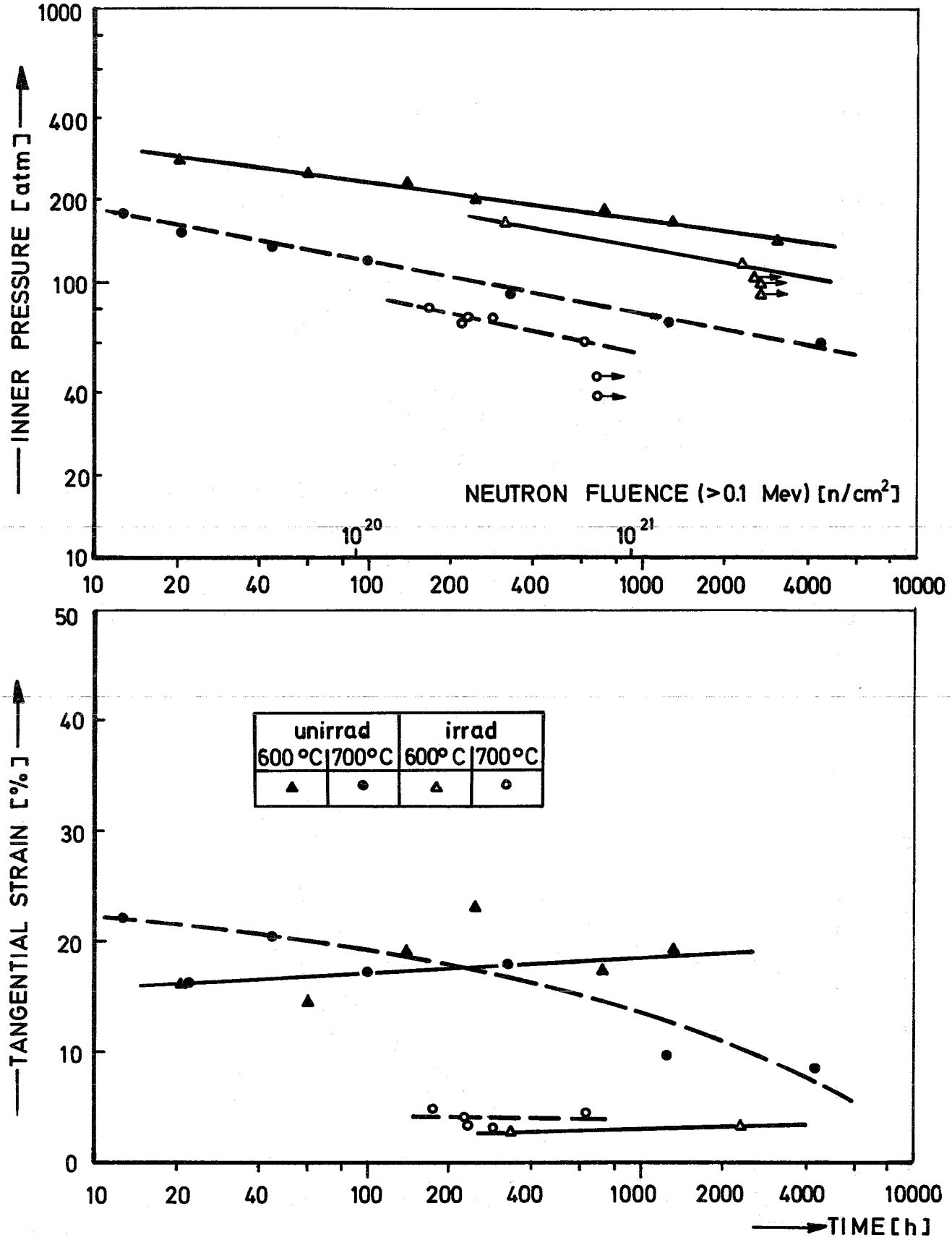

Fig.2 Stress rupture strength and tangential rupture strain of Incoloy 800 tubes

Outer diameter 7mm Wall thickness 0.4mm

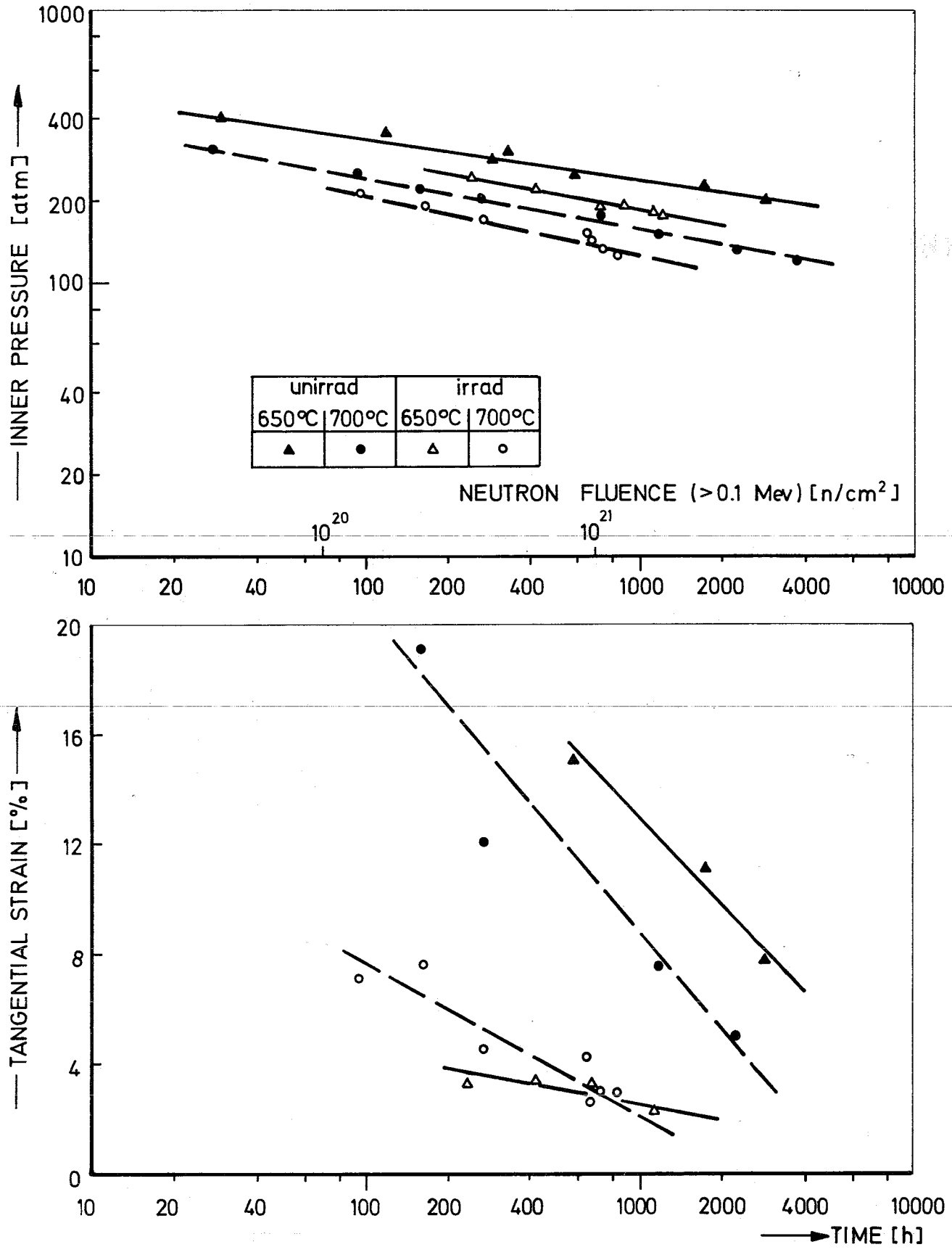

Fig.3 Stress rupture strength and tangential rupture strain of Hastelloy X tubes

Outer diameter 7mm Wall thickness 0.4 mm

Fig. 4
Program CRASH
Flow Chart

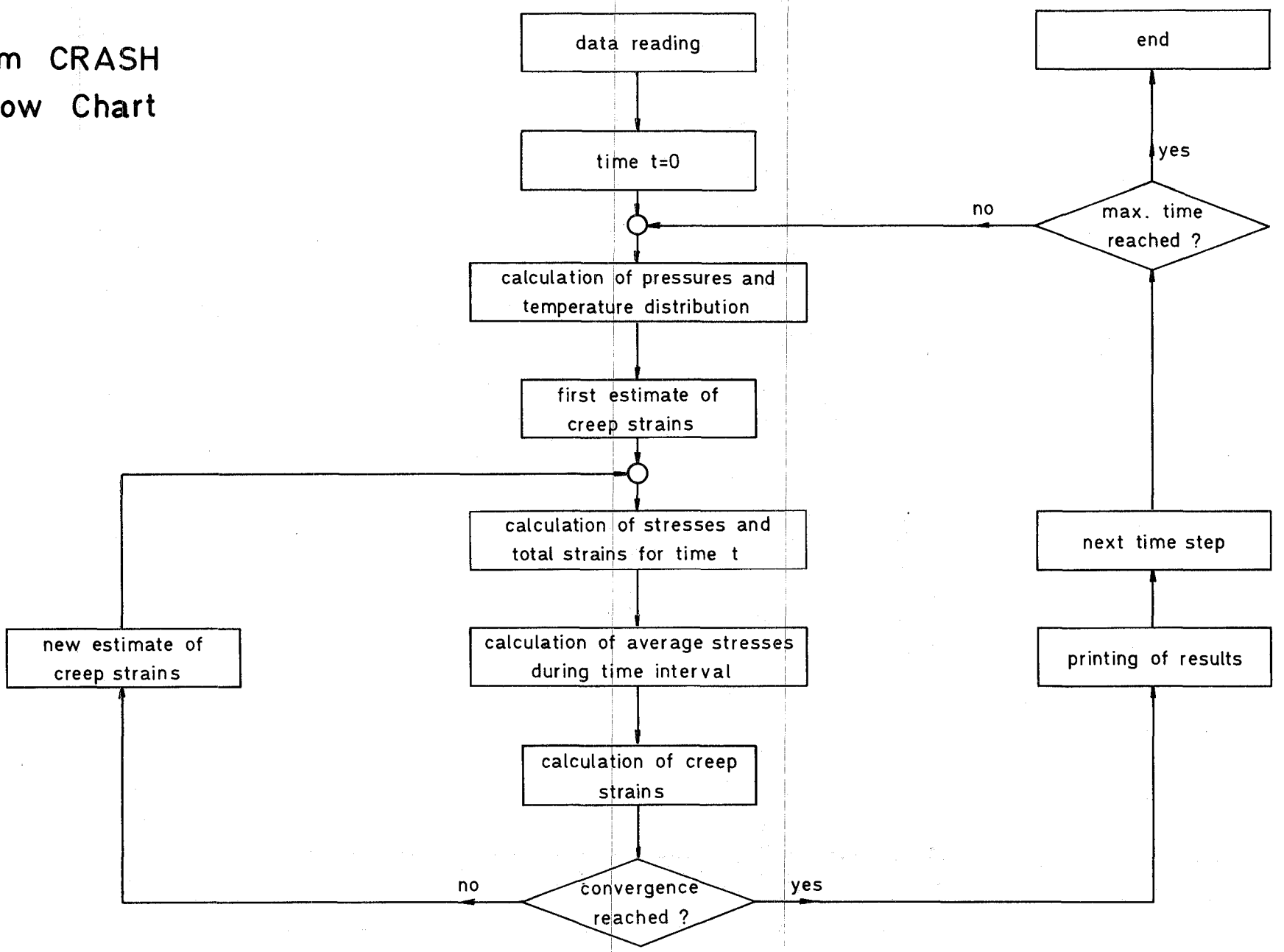

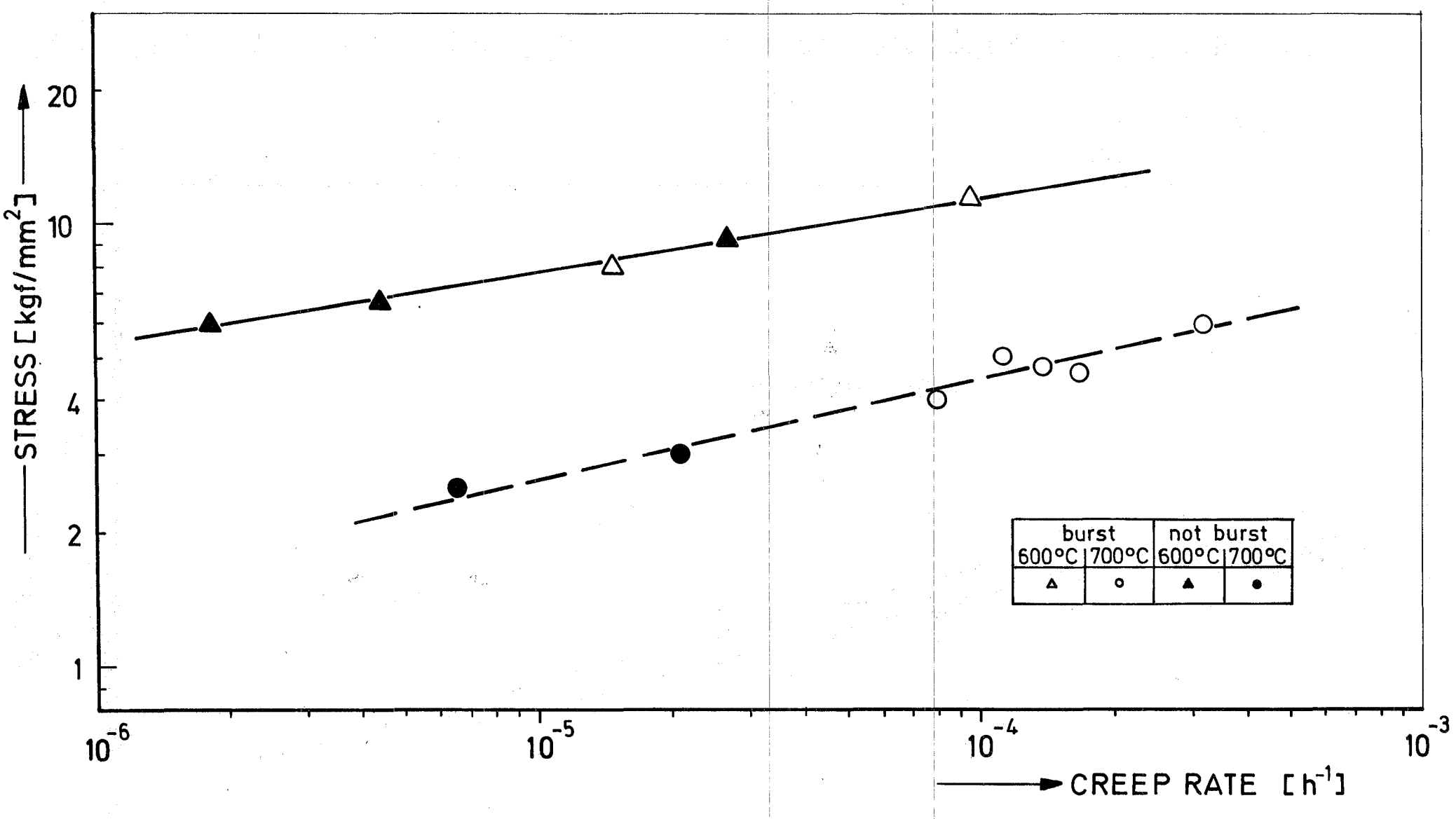

Fig.5 Variation of creep rate with stress level for irradiated Incoloy 800 tubes

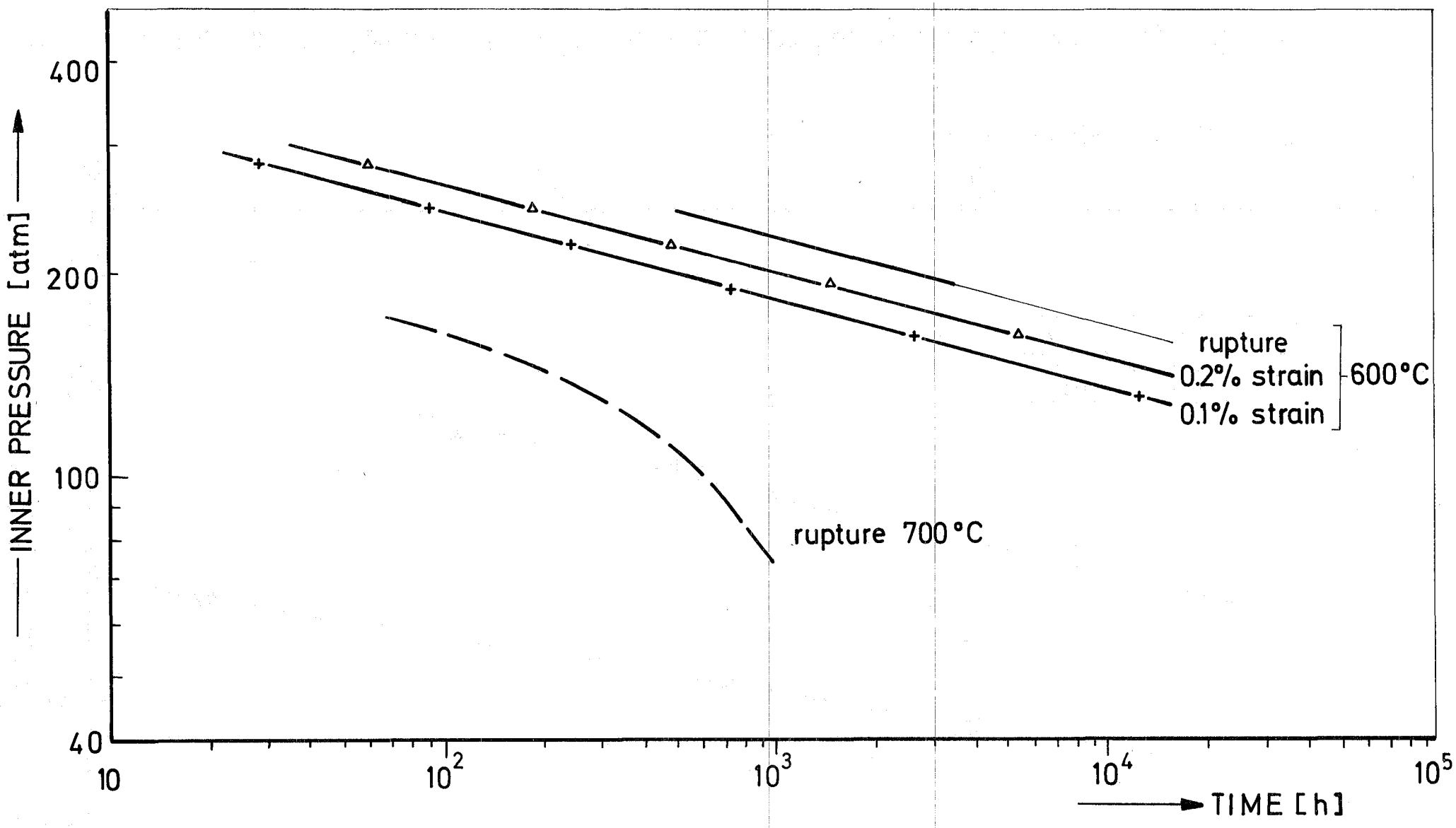

Fig.6 Stress rupture strength, 0.1% and 0.2% creep strength of irradiated 16Cr13Ni tubes

Outer diameter 6mm Wall thickness 0.38 mm

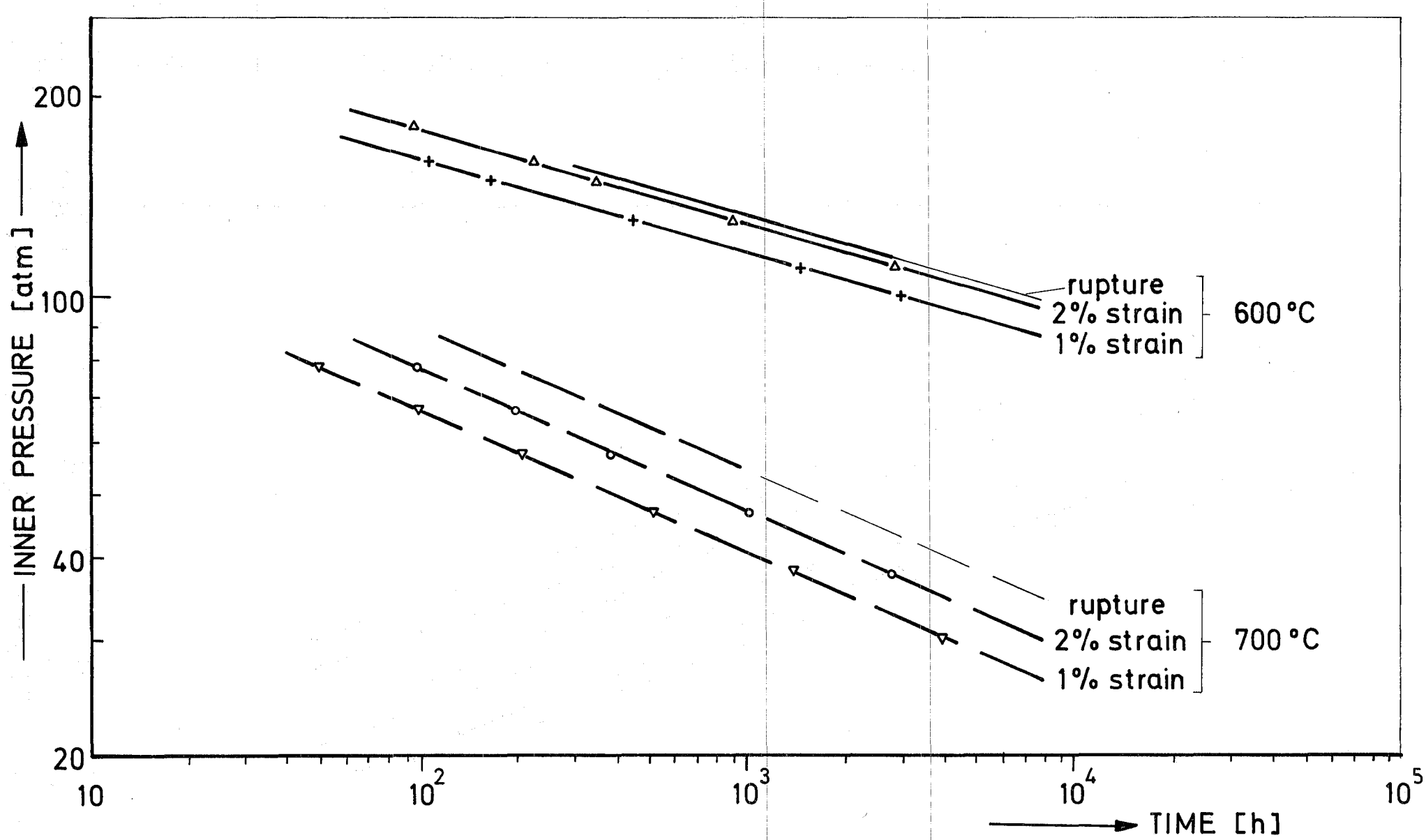

Fig.7 Stress rupture strength, 1% and 2% creep strength of irradiated Incoloy800 tubes

Outer diameter 7 mm Wall thickness 0.4 mm

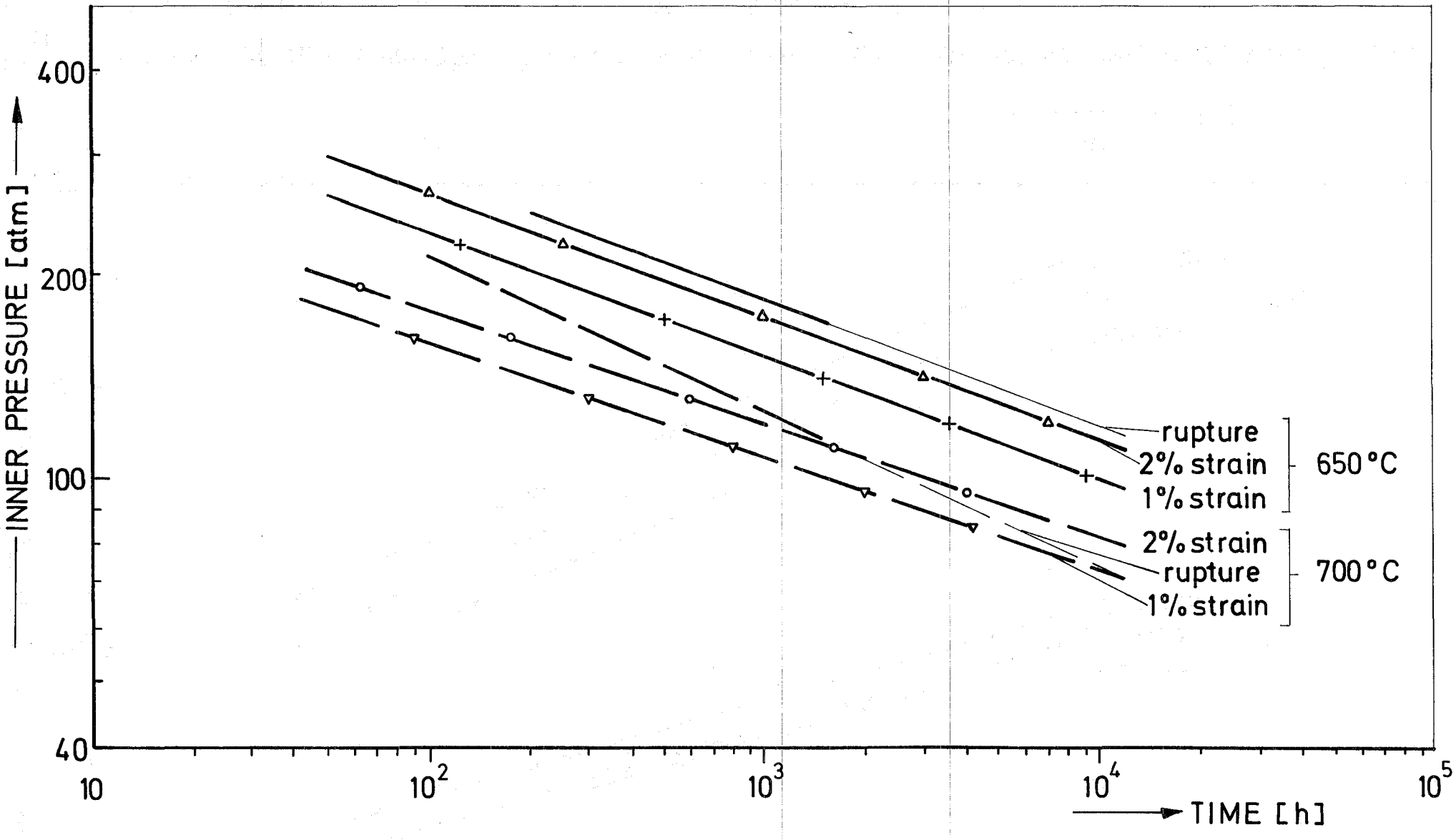

Fig. 8 Stress rupture strength, 1% and 2% creep strength of irradiated Hastelloy X tubes

Outer diameter 7 mm Wall thickness 0.4 mm

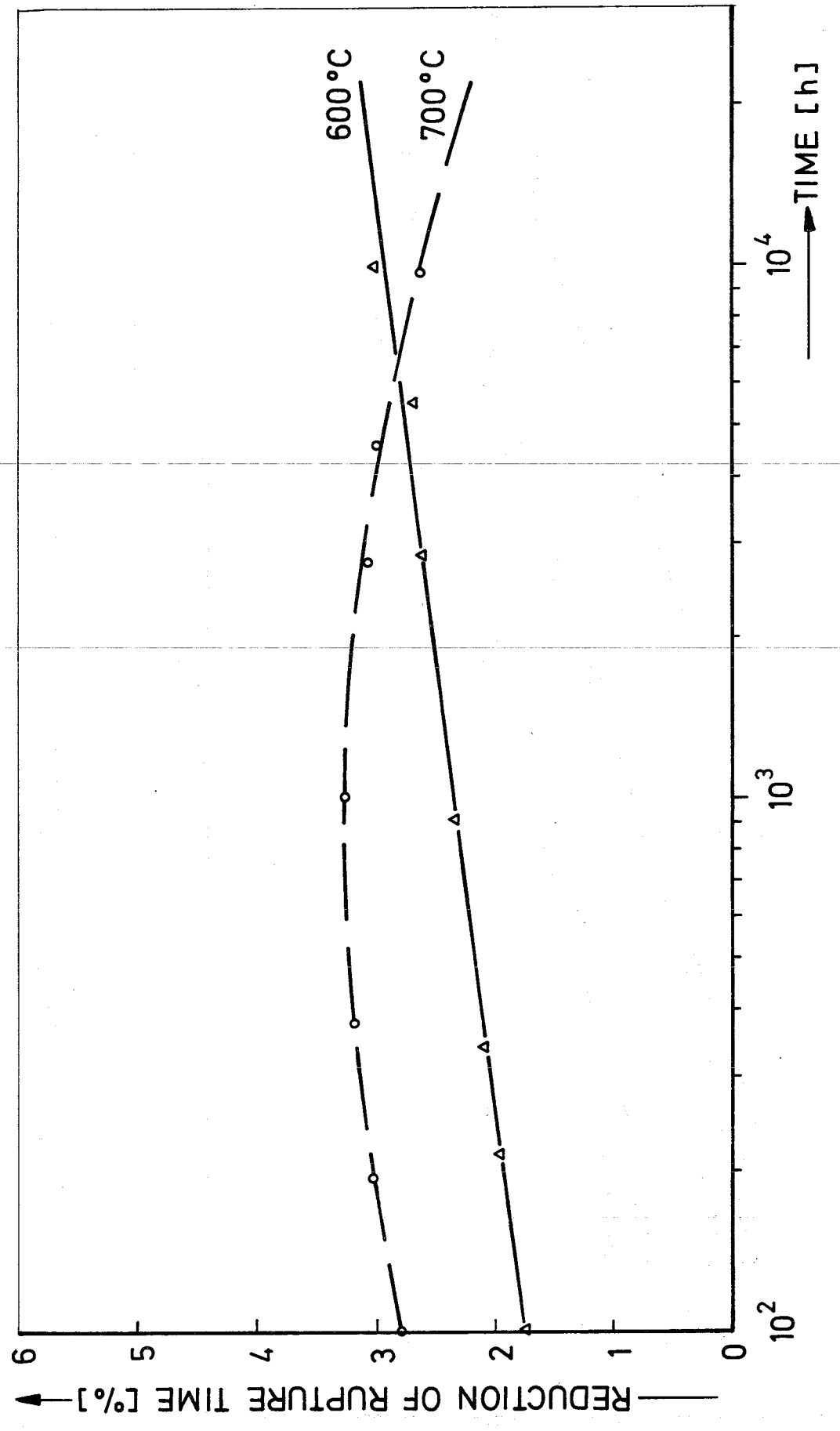

Fig. 9 Reduction of rupture time by thermal stresses for irradiated Incoloy 800 tubes

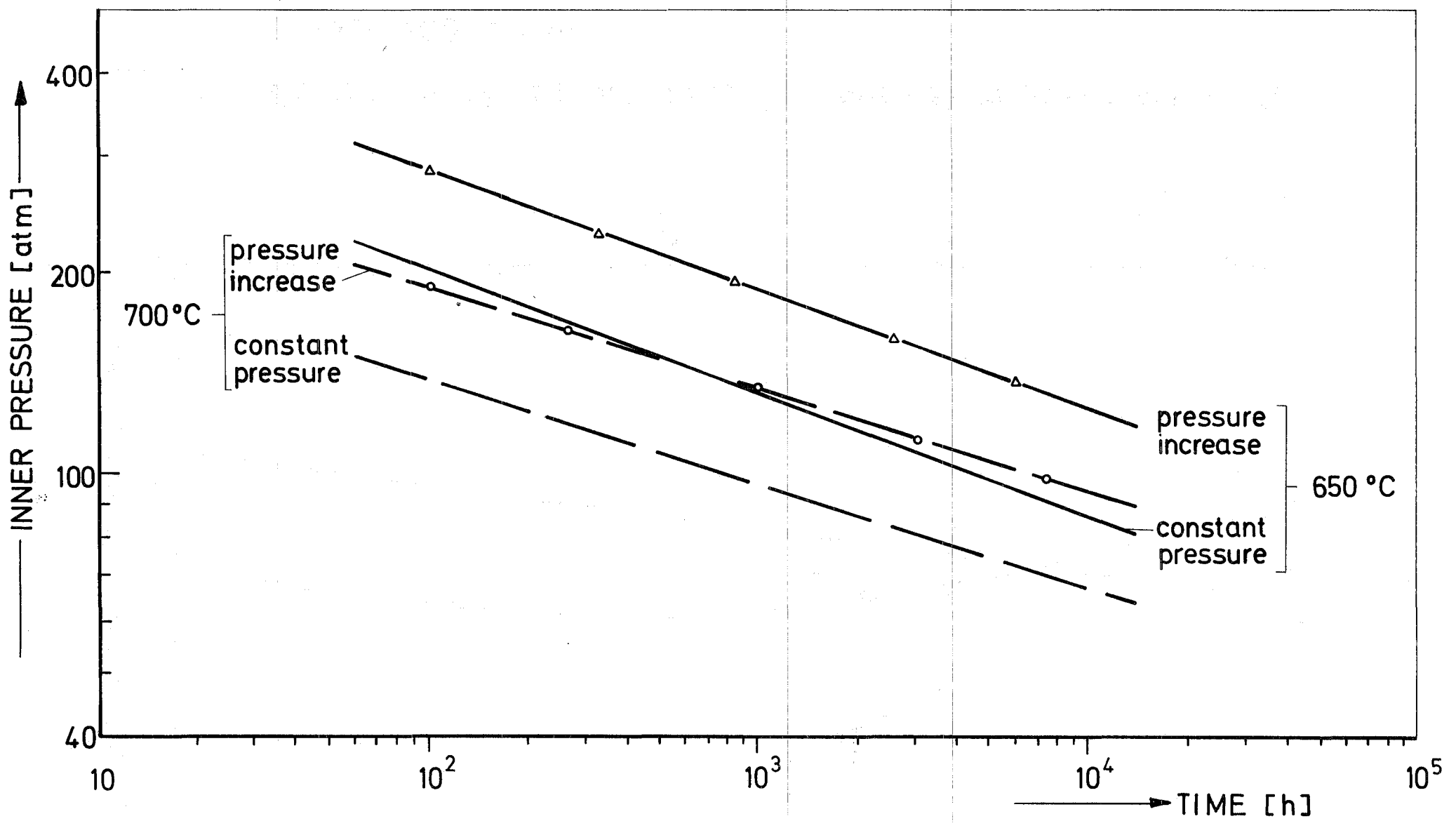

Fig. 10 0.5% creep strength of irradiated Hastelloy X tubes with pressure increase

Outer diameter 7mm Wall thickness 0.4 mm

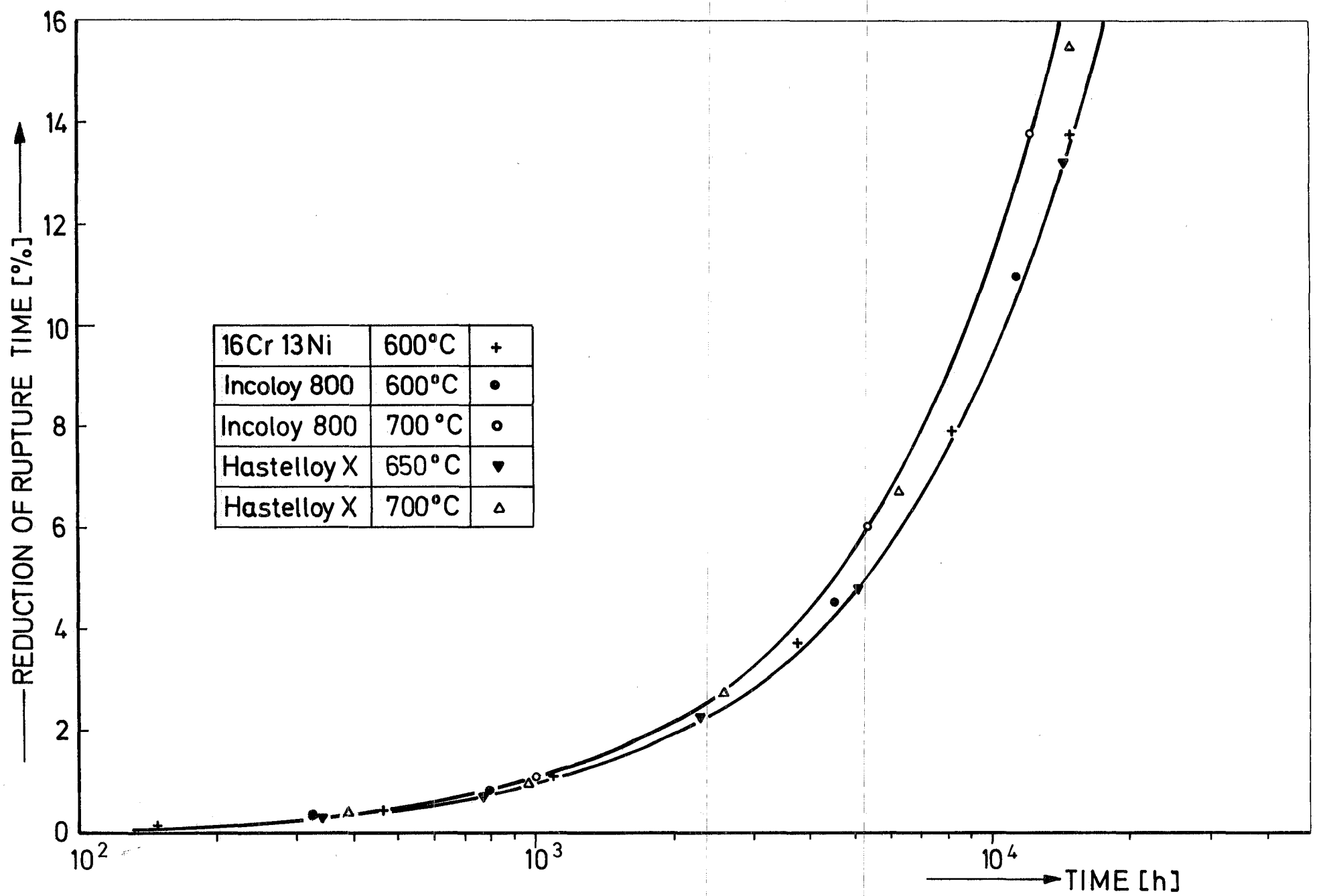

Fig. 11 Reduction of rupture time by corrosion. Corrosion rate 40 µm/a